

Improving Power System Stability Using Transfer Function: A Comparative Analysis

Ghazanfar Shahgholian

Department of Electrical Engineering
Najafabad Branch, Islamic Azad University
Najafabad, Iran
shahgholian@iaun.ac.ir

Arman Fattollahi

Smart Microgrid Research Center
Najafabad Branch, Islamic Azad University
Najafabad, Iran
fattollahi@iaun.ac.ir

Abstract—In this paper, a small-signal dynamic model of a single-machine infinite-bus (SMIB) power system that includes IEEE type-ST1 excitation system and PSS based on transfer function structure is presented. The changes in the operating condition of a power system on dynamic performance have been examined. The dynamic performance of the closed-loop system is analyzed base on its eigenvalues. The effectiveness of the parameters changes on dynamic stability is verified by simulation results. Three types of PSS have been considered for analysis: (a) the derivative PSS, (b) the lead-lag PSS or conventional PSS, and (c) the proportional-integral-derivative PSS. The objective function is formulated to increase the damping ratio of the electromechanical mode eigenvalues. Simulation results show that the PID-PSS performs better for less overshoot and less settling time compared with the CPSS and DPSS under different load operation and the significant system parameter variation conditions.

Keywords—power system stabilizer; PID controller; lead-lag controller; stability.

I. INTRODUCTION

Modern power systems are complex, nonlinear and often exhibit electromechanical oscillations due to inadequate system damping [1, 2]. Power systems continuously experience changes during abnormal operating conditions due to variations in generation or load and a wide range of disturbances. Power system stability improvements have been considered an important problem for secure system operation over many years [3, 4]. Low frequency electromechanical oscillations are a characteristic of the power system and they are inevitable. These oscillations can be observed in most power system variables like line current, bus voltage, synchronous generator power and speed. Generally, the damping control methods of power system oscillations can be divided into two broad groups: damping control at generator locations (such as excitation control) and damping control in the transmission path (such as line reactance control). Because of the complexity of the network evolved from the interconnected large transmission systems and heavy generations, the use of the power system stabilizer (PSS) has become common by the utilities today. PSS plays an important role to suppress the electromechanical oscillation, increase the system positive

damping and improve the steady-state stability margin and improve the stability in power system [5]. Generally, PSS control design methodologies can be categorized as (a) classical method, (b) adaptive and variable structure methods, (c) robust control approaches, (d) intelligent techniques and (e) digital control schemes [6, 7]. A number of studies have been performed about the PSS parameters design and its applications to improve the dynamic stability of power systems [8, 9]. An adaptive fuzzy PSS based on robust synergetic control theory and terminal attractor techniques is developed in [10], which fuzzy logic systems are used to approximate the unknown power system dynamic functions without calling upon usual model linearization and simplifications. In [11] a PSS designed using the improved simple adaptive control based on quadratic performance, which this approach can track the reference model and decrease the control increment. A method of designing fixed parameter decentralized PSS for interconnected multi-machine power systems is proposed in [12]. A technique for designing fixed parameter decentralized PSSs for interconnected power systems is proposed in [13], which local information available at each machine in the multi-machine environment, is used to tune parameters of PSS. A modified fruit fly optimization algorithm combined with a probabilistic approach to coordinate and optimize the parameters of PSS and SVC damping controller for improving the probabilistic small signal stability of power systems is proposed in [14]. A space recursive least square algorithm developed for tuning of PSS parameters on SMIB power system based PID is proposed in [15] to meet the vulnerable conditions. An objective function and algorithm to obtain a set of optimal PSS parameters that include a feedback signal of a remote machine and local and remote input signal ratios for each machine in a multi-machine power system under various operating conditions in proposed in [16]. A robust PID based PSS to properly function over a wide range of operating conditions is proposed in [17].

The objective of this paper is to investigate the effects of PSS based PID controllers on power system electromechanical oscillation damping. The synchronous generator is represented by the third-order model. The parameters of PSS are determined based on a linearized model of the power system around a nominal operating point where they can provided good performance. The effectiveness of the proposed PSS in

increasing the damping of low-frequency oscillation is demonstrated in a SMIB for different operating conditions of the power system.

II. POWER SYSTEM DESCRIPTION

Power system stabilizer is used to enhance damping of power system oscillations, mainly through excitation control. The IEEE type-ST1 is used for the voltage regulator excitation system [18]. The dynamic model in state-space form of the linearized SMIB power system model around an operation point can be expressed as [19]:

$$\frac{d}{dt} \Delta\delta = \omega_b \Delta\omega_r \tag{1}$$

$$\frac{d}{dt} \Delta\omega_r = -\frac{K_1}{J_M} \Delta\delta - \frac{D_I}{J_M} \Delta\omega_r - \frac{K_2}{J_M} \Delta E'_q + \frac{1}{J_M} \Delta T_M \tag{2}$$

$$\frac{d}{dt} \Delta E'_q = -\frac{K_4}{T'_{do}} \Delta\delta - \frac{1}{K_3 T'_{do}} \Delta E'_q + \frac{1}{T'_{do}} \Delta E_F \tag{3}$$

$$\frac{d}{dt} \Delta E_F = \frac{K_A}{T_A} \Delta U_R - \frac{K_A K_5}{T_A} \Delta\delta - \frac{K_A K_6}{T_A} \Delta E'_q - \frac{1}{T_A} \Delta E_F \tag{4}$$

where the state variables are angle load (δ), field voltage (E_F), angular velocity (ω_r) and voltage proportional to direct axis flux linkages (E'_q). Also, J_M is the generator inertia constant, D_I is the inherent damping constant, T'_{do} is the d-axis open circuit transient time constant, and ω_b is the base electrical angular velocity.

The primary inputs to the generating unit are the mechanical torque deviation (ΔT_M) and reference terminal voltage deviation (ΔU_R), which are supplied from a higher level of control. K_1 and K_2 are the constant derived from electrical torque, K_3 and K_4 are the constant derived from field voltage equation, and K_5 and K_6 are the constant derived from terminal voltage magnitude. The parameters K_1 - K_6 are constants for a particular operating point (PEO, QEO, UTO) but they are sensitive to power system network parameters and generator operating conditions. Figure 1 shows the functional block diagram of the SMIB power system based on control transfer function (between the output electrical torque and load angle), $H_Q(s)$, and the electrical loop transfer function (between exciter input and the output electrical torque), $GE(s)$. Also $GM(s)$ is the transfer function of the dynamic machine.

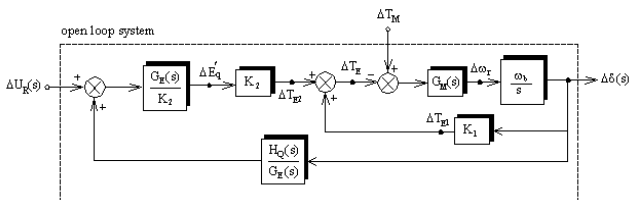


Fig. 1. Block diagram of the open loop SMIB power system based on control and electrical loop transfer functions

III. SYSTEM CONTROL SCHEME

A two-input two-output process be represented by the block diagram of the SMIB power system shown in Figure 2. The transfer functions $H_{ST}(s)$, $H_{TT}(s)$, $H_{SU}(s)$ and $H_{TU}(s)$ show the ratio output variables ω_r and T_E to input variables T_M and U_R in open loop system. When the speed deviation is used to input signal of PSS, the transfer function $H_{SU}(s)$ is important in PSS parameter design. But if electrical torque is used for PSS input signal, the transfer function $H_{TU}(s)$ is important in PSS parameter design. A system without PSS, will have:

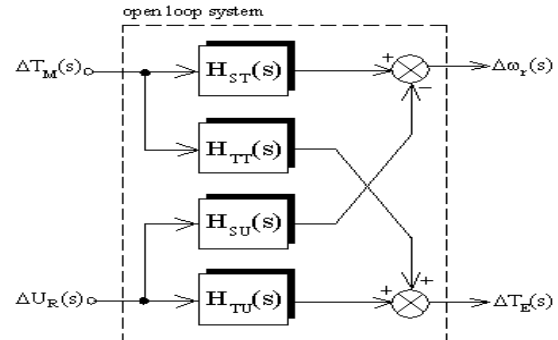


Fig. 2. Block diagram of the open loop SMIB power system based on transfer functions

$$H_{SU}(s) = \frac{\Delta\omega_r(s)}{\Delta U_R(s)} = \frac{1}{\Delta_O(s)} \frac{-K_2 K_A}{J_M T'_{do} T_A} s \tag{5}$$

$$H_{TU}(s) = \frac{\Delta T_E(s)}{\Delta U_R(s)} = \frac{1}{\Delta_O(s)} \frac{K_2 K_A}{T'_{do} T_A} s \left(s + \frac{D_I}{J_M} \right) \tag{6}$$

where $\Delta_O(s)$ is the open loop characteristic polynomial in power system. It has four eigenvalues. Therefore, the characteristic equation of the open loop SMIB power system is given by:

$$\Delta_O(s) = s^4 + p_3 s^3 + p_2 s^2 + p_1 s + p_0 \tag{7}$$

By varying the operating point, the coefficient parameter values p_0 through p_3 also vary.

A. Conventional Lead-Lag PSS

The conventional lead-lag PSS (CPSS) transfer function is given by the following [20]:

$$G_L(s) = K_C \frac{T_W s}{1 + T_W s} \left(\frac{1 + T_D s}{1 + T_G s} \right) \tag{8}$$

where T_W is the washout time constant and K_C is the PSS pure gain. T_D is the lead time constant and T_G is the lag time constant. The selection of the T_W value depends upon the type of mode under study [21]. Figure 3 show the phase frequency response characteristics of CPSS ($T_G=0.05$) according to the variation of T_D . The figure shows that the maximum phase lagging of the $G_L(s)$ happens on ω_C :

$$\omega_C \cong \frac{1}{\sqrt{T_D T_G}} \tag{9}$$

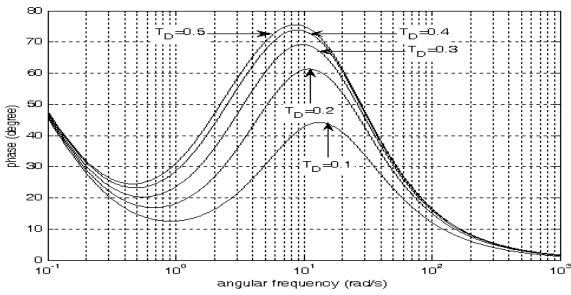


Fig. 3. Phase frequency response characteristics of the CPSS

B. Derivative PSS

The block diagram of the derivative power system stabilizer (DPSS) with gain K_d and time constant T_d used in this paper is depicted in Figure 4. The transfer function of the derivative PSS (DPSS) as shown in is given by:

$$G_D(s) = K_d \frac{T_d s}{1 + T_d s} \frac{T_d s}{1 + T_d s} \tag{10}$$

Bode plot of the DPSS for different values of T_d are shown in Figure 5. The Figure shows that the maximum amplitude of the $G_D(j\omega)$ at $\omega_m = 1/T_d$ is $K_d T_d / 2$. Also, in this frequency, the phase of the $G_D(j\omega)$ is zero. The time constant of the DPSS should optimally determine to compensate for phase lag between the exciter input and the generator electrical torque.

C. Proportional-Integral-Derivative PSS

A PID controller is commonly used by industrial utilities. It can be represented in transfer function form as [22, 23]:

$$G_C(s) = K_p + \frac{K_I}{s} + K_D s \tag{11}$$

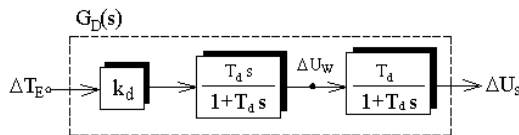


Fig. 4. The structures of a DPSS

Where K_p represents the proportional gain, K_I represents the integral gain, and K_D represents the derivative gain. The phase angle diagram of the PID controllers for different values of gains are shown in Figure 6. The PID-PSS as shown in Figure 7 with rotor deviation as input have the following transfer function:

$$G_P(s) = K_G \left(\frac{T_W s}{1 + T_W s} \right) \left(K_p + \frac{K_I}{s} + K_D s \right) \tag{12}$$

D. Close-Loop Transfer Function

The linearized model of the close-loop in a SMIB power system has six eigenvalues. The transfer functions in close loop system (with PSS) are given by the following:

$$H_{SV}(s) = \frac{\Delta\omega_r(s)}{\Delta U_R(s)} = \frac{-H_{SU}(s)}{1 + H_{SU}(s)G_P(s)} \tag{123}$$

$$H_{ER}(s) = \frac{\Delta T_E(s)}{\Delta U_R(s)} = \frac{H_{TU}(s)}{1 + H_{SU}(s)G_P(s)} \tag{134}$$

To increase the system damping, the eigenvalue-based objective function is considered as follows:

$$J = \max[\text{Real}(\lambda_i)] \tag{15}$$

where λ_i is the i^{th} electromechanical mode eigenvalue. In the optimization process, it is aimed to minimize J in order to shift the poorly damped eigenvalues to the left in s -plane.

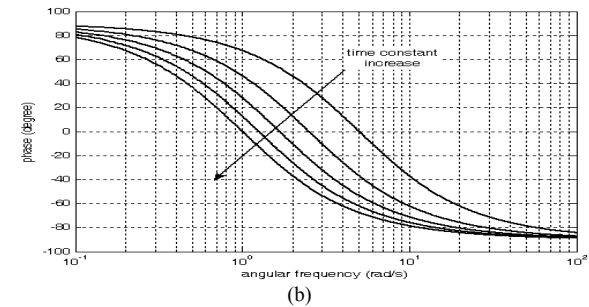
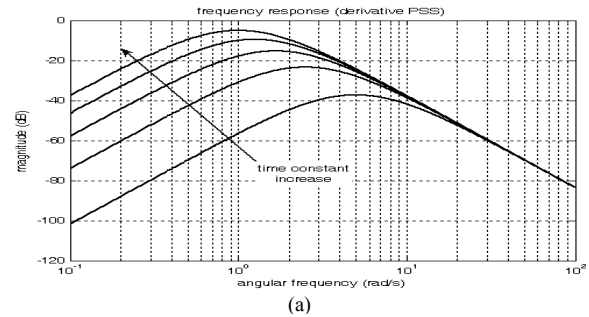


Fig. 5. Bode plot of the DPSS for various times constant

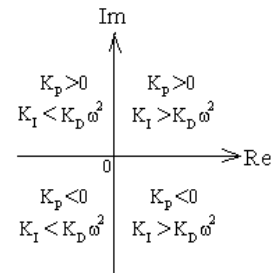


Fig. 6. Phase angle diagram of the PID controller

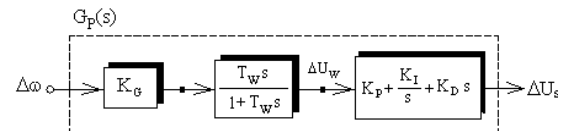


Fig. 7. Block diagram of PID power system stabilizer (PID-PSS)

E. Characteristic Equations

The characteristic equation of the close loop power system with DPSS s defined as:

$$\Delta_D(s) = s^6 + a_5s^5 + a_4s^4 + a_3s^3 + a_2s^2 + a_1s + a_0 \quad (16)$$

where the coefficients a_0 through a_6 are given by:

$$\begin{cases} a_5 = p_3 + \frac{2}{T_d} \\ a_4 = p_2 + \frac{2}{T_d} p_3 + \frac{1}{T_d^2} \\ a_3 = p_1 + \frac{2}{T_d} p_2 + \frac{1}{T_d^2} p_3 + K_d \frac{K_2 K_A}{T_A T_{do}} \\ a_2 = p_0 + \frac{2}{T_d} p_1 + \frac{1}{T_d^2} p_2 \\ a_1 = \frac{2}{T_d} p_0 + \frac{1}{T_d^2} p_1 \\ a_0 = \frac{1}{T_d^2} p_0 \end{cases} \quad (17)$$

According to this equation, all coefficients are depending on T_d , but a_3 only depend on the K_d . The characteristic equation of the close loop SMIB power system equipped with PID-PSS is given by:

$$\Delta_P(s) = s^5 + d_4s^4 + d_3s^3 + d_2s^2 + d_1s + d_0 \quad (18)$$

where the coefficients d_0 through d_4 are given by:

$$\begin{cases} d_4 = p_3 + \frac{1}{T_W} \\ d_3 = p_3 + \frac{p_2}{T_W} + \frac{K_G K_D K_2}{J_M T_{do}} \\ d_2 = p_2 + \frac{p_1}{T_W} + \frac{K_G K_P K_2}{J_M T_{do}} \\ d_1 = p_1 + \frac{p_0}{T_W} + \frac{K_G K_I K_2}{J_M T_{do}} \\ d_0 = \frac{p_0}{T_W} \end{cases} \quad (19)$$

The characteristic equation of the close loop SMIB power system equipped with CPSS is given by:

$$\Delta_L(s) = s^6 + m_5s^5 + m_4s^4 + m_3s^3 + m_2s^2 + m_1s + m_0 \quad (140)$$

where the coefficients m_0 through m_5 are given by the next equation according to which, the time constant T_1 only effected on m_3 and gain K_p only effected on m_3 and m_2 .

$$\begin{cases} m_5 = \frac{1}{T_W} + \frac{1}{T_2} + p_3 \\ m_4 = \frac{1}{T_W T_2} + p_3 \left(\frac{1}{T_W} + \frac{1}{T_2} \right) + p_2 \\ m_3 = \frac{p_3}{T_W T_2} + p_2 \left(\frac{1}{T_W} + \frac{1}{T_2} \right) + p_1 + \frac{K_A K_2}{J_M T_A T_{do}} \frac{K_P T_1}{T_2} \\ m_2 = \frac{p_2}{T_W T_2} + p_1 \left(\frac{1}{T_W} + \frac{1}{T_2} \right) + p_0 + \frac{K_A K_2}{J_M T_A T_{do}} \frac{K_P}{T_2} \\ m_1 = \frac{p_1}{T_W T_2} + p_0 \left(\frac{1}{T_W} + \frac{1}{T_2} \right) \\ m_0 = \frac{p_0}{T_W T_2} \end{cases} \quad (21)$$

IV. SIMULATION RESULTS

The small signal stability analysis of a SMIB power system is examined by the eigenvalues of the state matrix. To assess the effectiveness of the proposed controllers, three different loading conditions nominal, light and heavy as shown in Table I are considered for eigenvalue analysis. The data of the system is given in Table II. The constants K_1 to K_6 for the three operating points considered are given in Table III. Note that the constant K_5 is only positive for light loading. The system modes and damping ratio for electromechanical mode without PSS are given in Table IV. Note that the system without PSS is slightly damped only in light loading. The system response without applying any PSS is more oscillatory in heavy load condition. The maximum phase lagging of the open loop system in the $H_Q(s)$ is approximately -100 degree and in the $G_E(s)$ is approximately -140 degree at 10 rad/s, respectively. Therefore, one first-order blocks will be used to achieve the desired phase compensation. Also, the proportional and integral gains of PID controller are positive. The undamped natural angular frequency (ω_n) is $\omega_n=5.4741$ rad/s. The PSS parameters time-constants T_W , T_D , T_G and gain K_C are to be optimized. $T_W=10s$ and $T_G=0.05s$ are chosen. The required phase-lead can be obtained by choosing the value of time constant T_D . The transfer function $G_E(s)$ in the $j\omega_n$ is $1.2516\angle-62.9522^\circ$. Therefore, $T_D=0.8049s$ is obtained which provides the desired phase-lead of 62.9522° . The optimal parameters of the PSS base on phase compensation design are shown in Table V. The system eigenvalues with the stabilizer for three different operating conditions are given in Tables VI, VII and VIII. The damping ratio of the electrometrical mode eigenvalue for different loading of the power system without PSS and PSS are shown in Table IX.

TABLE I. DIFFERENT LOADING OPERATION

Normal load operation	$P_{E0}=0.8, Q_{E0}=0.6, U_{T0}=1$
Heavy load operation	$P_{E0}=1.3, Q_{E0}=1.0, U_{T0}=1$
Light load operation	$P_{E0}=0.3, Q_{E0}=0.1, U_{T0}=1$

TABLE II. SMIB POWER SYSTEM PARAMETERS

Generator	$J_M=10s, T'_{do}=6s, X_d=1.6, X'_d=0.32, X_q=1.55, f=50Hz$
IEEE type-ST1 excitation system	$K_A=50, T_A=0.05$
Transmission line Reactance	$R_E=0, X_E=0.4$

TABLE III. CONSTANTS K_1 - K_6 FOR DIFFERENT LOADING CONDITIONS

Parameters	Nominal loading	Light Loading	Heavy Loading
K_1	0.9538	0.7334	0.7803
K_2	0.9445	0.6526	1.0833
K_3	0.3600	0.3600	0.3600
K_4	1.2081	0.8353	1.3867
K_5	-0.0539	0.0573	-0.1989
K_6	0.4674	0.5154	0.4359

TABLE IV. SYSTEM MODES IN POWER SYSTEM WITHOUT PSS

Operating points	Mechanical mode	Electrical mode
Nominal loading	$0.1028 \pm j5.5022$	$-14.2975, -6.3710$
Light loading	$-0.1787 \pm j4.6571$	$-13.4839, -6.6216$
Heavy loading	$0.6068 \pm j5.3140$	$-14.4917, -7.1848$

TABLE V. OPTIMAL PARAMETERS SETTING FOR PSS

CPSS	$K_C=12.0458, T_W=10, T_D=0.8049, T_G=0.05$
PIDPSS	$K_G=1, T_W=10, K_P=19.4623, K_I=2.4753, K_D=11.2516$
DPSS	$K_d=2.03, T_d=0.30$

TABLE VI. SYSTEM MODES FOR POWER SYSTEM WITH PSS UNDER NORMAL LOADING

CPSS	PIDPSS	DPSS
$-1.5503 \pm j3.2201$	$-1.5376 \pm j3.1204$	$-1.3566 \pm j5.3300$
$-4.3234 \pm j11.4349$	$-8.6940 \pm j12.3729$	$-2.7562 \pm j4.6203$
-28.7149	-0.0997	-16.8229
-0.1007	0	-2.0811

TABLE VII. SYSTEM MODES FOR POWER SYSTEM WITH PSS UNDER HEAVY LOADING

CPSS	PIDPSS	DPSS
$-1.2608 \pm j3.3534$	$-1.2518 \pm j3.2023$	$-0.4622 \pm j5.1017$
$-4.2564 \pm j11.7692$	$-8.9798 \pm j13.1208$	$-3.4194 \pm j4.8032$
-29.4278	-0.0997	-17.2650
-0.1007	0	-2.1013

TABLE VIII. SYSTEM MODES FOR POWER SYSTEM WITH PSS UNDER LIGHT LOADING

CPSS	PIDPSS	DPSS
$-1.3208 \pm j3.0888$	$-1.3473 \pm j2.9787$	$-0.4622 \pm j5.1017$
$-5.3531 \pm j9.8632$	$-8.8843 \pm j10.1524$	$-3.4194 \pm j5.1017$
-27.1145	-0.0997	-17.2650
-0.1006	0	-2.1013

A comparative between the conventional PSS and DPSS with PIDPSS in damping power system oscillation under normal operating conditions is shown in Figures 8, 9 and 10. The step response of the angular speed deviation under heavy operating conditions has been shown in Figure 11. The results show the superiority of PIDPSS and CPSS over DPSS in increasing the damping of low frequency oscillations. Table X shows the summary of the system dynamic characteristics such as settling time (t_s), peak time (t_p) and percent overshoot (M_p). It is seen from these simulation studies that the PID-PSS is more effective than the CPSS and DPSS in damping the electromechanical oscillations under various loading conditions and its damping speed is much faster.

TABLE IX. DAMPING RATIO OF ELECTROMECHANICAL MODE FOR POWER SYSTEM UNDER DIFFERENT OPERATION CONDITIONS

Loading	Without PSS	CPSS	DPSS	PIDPSS
Normal loading	-0.0187	0.4338	0.2467	0.4420
Heavy loading	-0.1135	0.3519	0.0902	0.3641
Light loading	0.0383	0.3932	0.0902	0.4121

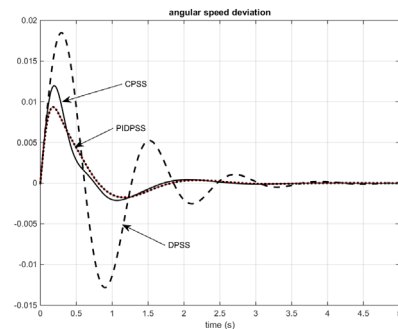


Fig. 8. Step response of the angular speed deviation

V. NONLINEAR SIMULATION

The scenario was simulated that a 0.10 pu step change in the input mechanical power occurred at 0 s. The simulation results are shown in Figures 12-14. The simulation results show that the PID-PSS achieved better damping effects than the derivative PSS and conventional PSS.

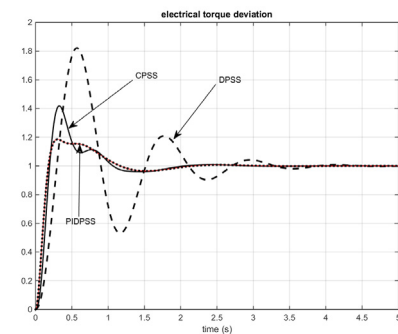


Fig. 9. Step response of the electrical torque deviation

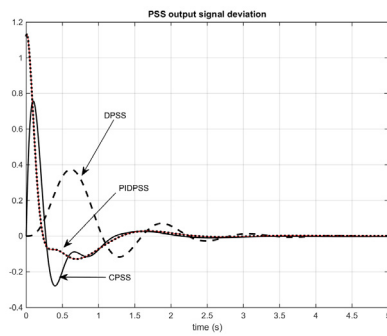


Fig. 10. Step response of the PSS output signal deviation

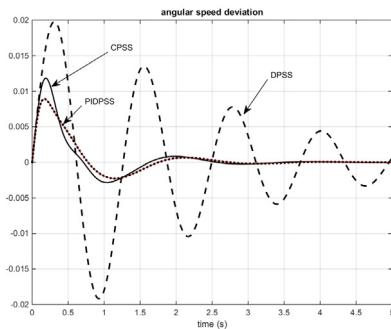


Fig. 11. Step response of the angular speed deviation under heavy loading

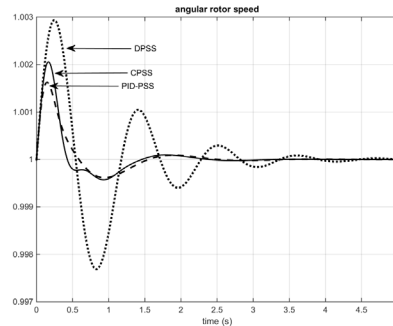


Fig. 13. Rotor speed response to a 10% mechanical power change

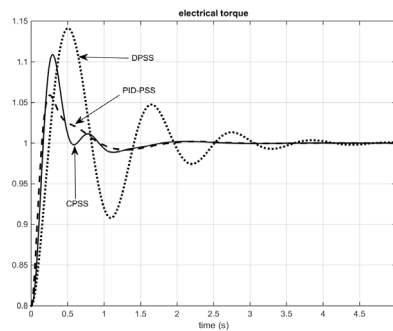


Fig. 14. Electrical power response to a 10% mechanical power change

TABLE X. SYSTEM DYNAMIC CHARACTERISTIC

PSS	t_s	t_p	$M_p\%$
CPSS	7.9621	1.2576	106.8231%
DPSS	2.6399 s	0.6156 s	126.5998%
PIDPSS	1.9988	0.8094	126.2119%

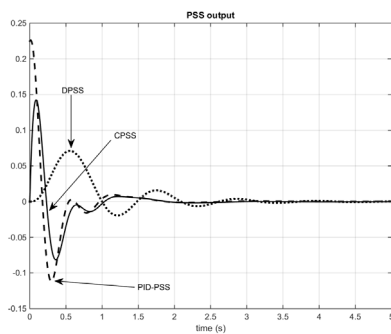


Fig. 12. PSS output response to a 10% mechanical power change

VI. CONCLUSION

The main function of power system stabilizer is suppressing the low-frequency oscillation of the power system to improve its dynamic stability. The dynamic response of a SMIB power system with PSS based on transfer function at various operating conditions has been investigated in this paper. Three types of PSS have been considered for analysis. The PID-PSS

performs better for less overshoot and less settling time compared with the CPSS and DPSS under different load operation and the significant system parameter variation conditions.

REFERENCES

- [1] G. Shahgholian, M. Maghsoodi, A. Movahedi, "Fuzzy proportional integral controller desing for thyristor controlled series capacitor and power system stabilizer to improve power system stability", *Revue Roumaine Des Sciences Techniques*, Vol. 61 No. 4, pp. 418-423, 2016
- [2] G. Shahgholian, K. Khani, M. Moazzami, "Frequency control in autonomous microgrid in the presence of DFIG based wind turbine", *Journal of Intelligent Procedures in Eleectrical Technology*, Vol. 6 No. 23, pp. 3-12, 2015
- [3] G. Shahgholian, A. Movahedi, J. Faiz, "Coordinated design of TCSC and PSS controllers using VURPSO and genetic algorithms for multi-machine power system stability", *International Journal of Control, Automation, and Systems*, Vol. 13, No. 2, pp. 398-409, 2015
- [4] G. Shahgholian, A. Movahedi, "Power system stabiliser and flexible alternating current transmission systems controller coordinated design using adaptive velocity update relaxation particle swarm optimisation algorithm in multi-machine power system", *IET Generation, Transmission & Distribution*, Vol. 10, No. 8, pp. 1860-1868, 2016
- [5] G. Shahgholian, "Review of power system stabilizer: Application, modeling, analysis and control strategy", *International Journal on Technical and Physical Problems of Engineering*, Vol. 5, No. 3, pp. 41-52, 2013
- [6] E. Gholipour, S. M. Nosratabadi, "A new coordination strategy of SSSC and PSS controllers in power system using SOA algorithm based on Pareto method", *International Journal of Electrical Power and Energy Systems*, Vol. 67, pp. 462-471, 2015
- [7] R. K. Khadanga, J. K. Satapathy, "Time delay approach for PSS and SSSC based coordinated controller design using hybrid PSO-GSA

- algorithm", International Journal of Electrical Power and Energy Systems, Vol. 71, pp. 262-273, 2015
- [8] C. Pradhan, C. N. Bhende, "Frequency sensitivity analysis of load damping coefficient in wind farm-integrated power system sign in or purchase", IEEE Transactions on Power Systems, Vol. 32, No. 2, pp. 1016-1029, 2017
- [9] G. Shahgholian, A. Movahedi, "Coordinated design of thyristor controlled series capacitor and power system stabilizer controllers using velocity update relaxation particle swarm optimization for two-machine power system stability", Revue Roumaine Des Sciences Techniques, Vol. 59, No. 3, pp. 291-301, 2014
- [10] Z. Bouchama, N. Essounbouli, M. N. Harmas, A. Hamzaoui, K. Saoudi, "Reaching phase free adaptive fuzzy synergetic power system stabilizer", International Journal of Electrical Power and Energy Systems, Vol. 77, pp. 43-49, 2016
- [11] S. Zhang, F. L. Luo, "An improved simple adaptive control applied to power system stabilizer", IEEE Transactions on Power Electronics, Vol. 20, No. 2, pp. 369-375, 2009
- [12] G. Guraala, I. Sen, "Power system stabilizers design for interconnected power systems", IEEE Transactions on Power Systems, Vol. 25, No. 2, pp. 1042-1051, 2010
- [13] A. Kumar, "Power system stabilizers design for multimachine power systems using local measurements", IEEE Transactions on Power Systems, Vol. 31, No. 3, pp. 2163-2171, 2016
- [14] X. Y. Bian, Y. Geng, K. L. Lo, Y. Fu, "Coordination of PSSs and SVC damping controller to improve probabilistic small-signal stability of power system with wind farm integration", IEEE Transactions on Power Systems, Vol. 31, No. 3, pp. 2371-2382, 2016
- [15] A. Ragavendiran, R. Gnanadass, K. Ramakrishnan, "A new SPARLS algorithm for tuning power system stabilizer", International Journal of Electrical Power and Energy Systems, Vol. 68, pp. 327-335, 2015
- [16] S. K. Wang, "A novel objective function and algorithm for optimal PSS parameter design in a multi-machine power system", IEEE Transactions on Power Systems, Vol. 28, No. 1, pp. 522-531, 2013
- [17] M. Solimana, A. L. Elshafei, F. Bendarya, W. Mansoura, "Robust decentralized PID-based power system stabilizer design using an ILMI approach", Electric Power Systems Research, Vol. 80, pp. 1488-1497, 2010
- [18] K. Bhattacharya, J. Nanda, M. L. Kothari, "Optimization and performance analysis of conventional power system stabilizers", International Journal of Electrical Power and Energy Systems, Vol. 19m, No. 7, pp. 449-458, 1997
- [19] G. Shahgholian, "Development of state space model and control of the STATCOM for improvement of damping in a single-machine infinite-bus", International Review of Electrical Engineering, Vol. 4, No. 6, pp. 1367-1375, 2009
- [20] T. R. Jyothsna, K. Vaisakh, "Effects of strong resonance in tuning of multiple power system stabilizers", IET Generation, Transmission and Distribution, Vol. 5, No. 11, pp. 1155-1164, 2011
- [21] O. M. Awed-Badeeb, "Damping of electromechanical modes using power system stabilizers case: electrical Yemeni network", Journal of Elecectrical Engineering, Vol. 57, No. 5, pp. 291-295, 2006
- [22] G. Shahgholian, A. Rajabi, B. Karimi, "Analysis and design of PSS for multi-machine power system based on sliding mode control theory", International Review of Electrical Engineering, Vol. 4, No. 2, pp. 2241-2250, 2010
- [23] G. Shahgholian, "Power system stabilizer application for load frequency control in hydro-electric power plant", Engineering Mathematics, Vol. 2, No. 1, pp. 21-30, 2017